MODELLING AND ANALYSIS OF ENERGY-EFFICIENT HEAT TRANSFER PROCESSES IN NON-LINEAR STRUCTURED FLUIDS OF GROUND HEAT EXCHANGERS IN HEAT PUMP HEATING SYSTEMS OF INDOOR SPORTS FACILITIES

Yurii Chovniuk, Anna Moskvitina, Serhii Rybachov, Petro Zinych
Kyiv National University of Construction and Architecture, Ukraine
chovniuk.iuv@knuba.edu.ua, moskvitina.as@knuba.edu.ua, rybachov.sg@knuba.edu.ua

Abstract. The work uses the Green's function method to solve the three-dimensional convective wave equation for a straight channel of a ground heat exchanger of arbitrary but constant cross-sectional shape, which models the propagation of thermoacoustic wave formations in the specified channel. In this case, the channel walls can be acoustically rigid, acoustically soft, or have mixed acoustic properties. The Green's function is represented by a series of acoustic modes of the channel. Each member of the series is, in turn, a superposition of forward and backward waves propagating in the corresponding mode down and up the heat carrier flow from a single point impulse acoustic source. In such a constructed model of thermoacoustic excitations of the ground heat exchanger channel using the Green's function, the effects of uniform averaged flow in the channel of a nonlinear structured heat carrier are reflected. In the absence of flow in the heat exchanger channel, the Green's function is symmetric with respect to the specified cross-section. Based on this approach, Green's functions of the three-dimensional convective wave equation for straight channels of a ground heat exchanger with a circular cross-section were obtained. The use of a special transformation allows the reduction of the one-dimensional Klein-Gordon convective equation to its classical one-dimensional analogue, which has a known solution. Within the framework of models for describing the rheological properties of nonlinear viscoplastic fluids, which combine plasticity and anomalous viscosity in a nonlinear degree, it is possible to use them directly in momentum and energy transfer equations. The energy efficiency of using tubular ground heat exchangers for highly viscous heat transfer fluids (e.g., propylene glycol-based nanofluids) and the influence of structural nonlinearity on the Nusselt number during the operation of such energy-saving systems in indoor sports facilities have been determined.

Keywords: heat pump systems, energy efficiency, microclimate, heat and mass transfer, non-linear structured fluid carriers, microclimate control systems for sports facilities, thermoacoustic wave generation.

Introduction

The study of thermal and thermoacoustic fields in ducts of various geometries is of great interest to the utilities sector. This is especially true for ground-source heat exchangers used in heat pump heating systems of indoor sports facilities [1-3]. Such systems provide energy-efficient operation of buildings. All these problems are fundamentally solved using the Green's function method [4]. However, deriving this function is a difficult task. It depends on many factors: channel geometry, cross-section shape, wall properties, external and internal environments, acoustic conditions, initial and boundary conditions, as well as flows inside the channel and in the surrounding soil. In most previous studies, the Green's function for the wave and Helmholtz equations was derived without considering fluid flow [5; 6]. At the same time, for ground heat exchangers the effects of internal heat carrier flow and external soil movement (landslides, groundwater) play a key role. This is particularly important when using a hyperbolic heat conduction model that accounts for the finite speed of heat propagation. In this study, previous results on the Green's function for the hyperbolic heat conduction equation are developed and generalized. For the first time, the influence of both the internal flow of the heat transfer fluid and the movement of the surrounding soil is explicitly taken into account. A straight channel with a circular cross-section is considered as a model. The resulting temperature fields clearly depend on the flow parameters inside the channel and outside it. A hyperbolic heat conduction model is used [7; 8].

In earlier works [9-11], the effect of flow on the Green's function was considered mainly implicitly. This shortcoming was partially addressed in publications [12-14], where the Green's function was derived for an infinite rigid-walled channel with uniform internal flow (circular and rectangular cross-sections). Author [15] further developed these results, but studied only acoustic fields. For thermal fields in the hyperbolic transport model that simultaneously accounts for both internal coolant flow and external soil flow, similar studies have not been conducted before.

The aim of this work is to justify the algorithm for constructing the Green's function of the three-dimensional convective wave equation for a straight circular channel of a ground heat exchanger. This is done to model and analyze energy-efficient heat and mass transfer processes in nonlinear structured

heat transfer fluids, taking into account internal and external flows within the hyperbolic transport model.

Materials and methods

Heat pumps with ground-source heat exchangers provide low-temperature heating for indoor sports facilities by utilizing the stable, low-grade heat of the ground. Such systems are particularly effective for maintaining the indoor climate in sports halls (temperature 18-22 °C), reducing energy costs by 40-60% compared to traditional heating and improving the energy efficiency of buildings in rural areas. The efficiency of heat pump systems directly depends on heat transfer processes in the ground heat exchanger-storage unit, from which the heat pump extracts heat and transfers it to the heating circuit. Standard calculations for ground-based heat exchangers in heat pump heating systems include calculations based on the average heat flow per 1 m^2 or 1 m^3 [1; 8; 9]. However, full hydrodynamic and thermal calculations of the heat exchanger are not performed. To accurately analyze these processes, this study applies the Green's function method to the three-dimensional convective wave equation, taking into account the internal flow of a nonlinearly structured heat transfer fluid.

In this study, a hyperbolic heat conduction equation was derived that accounts for the flow of a heat-carrying fluid in a cylindrical pipe with a circular cross-section, which moves along its horizontal axis Oz at a velocity $\vec{U}$ (Fig. 1). The magnitude of this velocity is determined by the rheological model of the heat transfer fluid itself and the assumed boundary conditions on the pipe walls. Additionally, the motion of the surrounding soil of the heat exchanger – the soil medium – at a velocity $\vec{v}$ is taken into account, which creates an additional external heat flux $\vec{q}$ on the pipe surface.

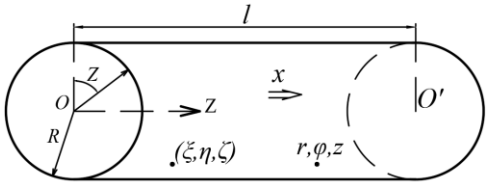

Fig. 1. **Finite straight channel with a circular cross-section and length *l***

The solution of the hyperbolic heat conduction equation was obtained in a cylindrical coordinate system using the Green's function method. This solution is based on the hyperbolic theory of heat conduction, which takes into account the finite speed of heat propagation. It allows more accurate determination of strength standards for ground heat exchanger pipelines during system startup, shutdown, and flow reversal (for maintenance, repairs, and diagnostics). It also helps optimize heat extraction and transfer modes without disrupting the normal operation of buildings and structures [16]. Based on the hyperbolic Fourier–Lykov law with the thermal relaxation time τ_r, and considering both soil movement and internal coolant flow, a non-homogeneous Klein–Gordon equation in cylindrical coordinates (r, φ, z) was derived [6; 7; 16]. To account for internal flow, a convective substitution of time-derivative operators was performed, and the thermal Mach number was introduced:

$$\frac{U}{v_{\mathrm{t}}} = M \tag{1}$$

and the transition to dimensionless variables has been made:

$$\frac{\partial^2 \Theta}{\partial \bar{T}^2} = v_T^2 \cdot \left[\frac{1}{\mathrm{r}} \cdot \frac{\partial}{\partial \mathrm{r}}\left(r \cdot \frac{\partial \Theta}{\partial r}\right) + \frac{1}{r^2} \cdot \frac{\partial^2 \Theta}{\partial \varphi^2} + \frac{\partial^2 \Theta}{\partial \bar{z}^2}\right] + \bar{\Phi}(r, \varphi, \bar{z}, \bar{t}) \tag{2}$$

where T – temperature of the coolant, °C.

This allowed the equations to be reduced to their classical form without convective terms. The solution to the equations was obtained using the Green's function method for a finite circular cylinder under various boundary conditions, typical for real operating conditions of ground heat exchangers. Next, a circular cylinder of finite length l is considered. Since

$$T(r, \varphi, z, t) = \theta(r, \varphi, z, t)\exp(-t/(2\tau_r)),$$

then, by specifying the boundary and initial conditions for $\theta(r, \varphi, z, t)$, the corresponding boundary and initial conditions for the true temperature $T(r, \varphi, z, t)$ can be found using the given exponential transformation. The methodology for calculating transport systems and the optimal design of tubular heat exchangers was originally implemented by the author in the FORTRAN programming language. We modified these programs and switched to the MATHCAD algorithmic language [4; 5; 16].

To analyze the influence of the coolant's rheological properties on the average flow velocity U, several models of non-Newtonian fluids were considered: the Shvedov–Bingham model, the Ostwald–de Villiers (power-law) model, the Ellis model, and the model of a fluid with structural viscosity. For each model, the average flow velocity was determined and the heat transfer intensity (Nusselt numbers) was evaluated under laminar flow conditions, including non-isothermal flow. For structurally viscous fluids, the heat transfer process was analyzed in the boundary layer near the pipe wall.

Results and discussion

Green's functions for various boundary value problems. The domain is $0 \le r \le R$, $0 \le \varphi \le 2\ \pi$, $0 \le \overline{z} \le l$. The first boundary value problem. The following conditions are given:

$$\begin{cases} \Theta\ =\ f_0(r,\varphi,\bar{z}) \text{ when } \bar{T}\ =\ 0;\ \dfrac{\partial\ \Theta}{\partial \bar{T}}\ =\ f_1 \cdot (r,\varphi,\bar{z}) \text{ when } \bar{T}\ =\ 0; \\ \Theta\ =\ g_1(\varphi,\bar{z},\bar{T}) \text{ when } r\ =\ R;\ \Theta\ =\ g_2 \cdot (\varphi,r,\bar{T}) \text{ when } \bar{Z}\ =\ 0; \\ \Theta\ =\ g_3(r,\varphi,\bar{T}) \text{ when } \bar{Z}\ =\ l \end{cases} \quad (3)$$

Here, the Green's function takes the following form:

$$G(r,\varphi,\bar{Z},\xi,\eta,\zeta,\bar{T})\ =\ \frac{2}{\pi R^2 l} \cdot \sum_{n\,=\,0}^{\infty} \sum_{m\,=\,1}^{\infty} \sum_{k\,=\,1}^{\infty} \frac{A_n \cdot I_n(\mu_{nm} r)\ \cdot I_n(\mu_{nm}\xi)}{[I_n'(\mu_{nm} R)]^2 \sqrt{\lambda_{nmk}}} \text{x}$$

$$\text{x}\ cos[n \cdot (\varphi - \eta)] \cdot \sin\left(\frac{k\pi\bar{Z}}{l}\right) \cdot \sin\left(\frac{kn\zeta}{l}\right) \cdot \sin\left(\bar{T} \cdot \sqrt{\lambda_{nmk}}\right), \quad (4)$$

where $\lambda_{nmk}\ =\ v_t^2 \cdot \mu_{nm}^2\ +\ \dfrac{v_t^2 \cdot k^2 \cdot \pi^2}{l^2}\ +\ b, \mathrm{A}_n\ =\ \begin{cases} 1 \text{ when } n\ =\ 0, \\ 2 \text{ when } n\ >\ 0, \end{cases}$

$I_n(\xi)$ – Bessel function of the argument (ξ); the bar above the function denotes the derivative with respect to that specific argument;

μ_{nm} – positive roots of the transcendental equation $I_n(\mu R) = 0$.

The domain is $0 \le r \le R$, $0 \le \pi \le 2\ \pi$, $0 \le \overline{z} \le l$. Second boundary value problem. The following conditions are given:

$$\begin{cases} \Theta\ =\ f_0(r,\varphi,\bar{z}) \text{ when } \bar{T}\ =\ 0;\ \dfrac{\partial\ \Theta}{\partial \bar{T}}\ =\ f_1 \cdot (r,\varphi,\bar{z}) \text{ when } \bar{T}\ =\ 0; \\ \dfrac{\partial\ \Theta}{\partial r}\ =\ g_1(\varphi,\bar{z},\bar{T}) \text{ when } r\ =\ R;\ \dfrac{\partial\ \Theta}{\partial \bar{Z}}\ =\ g_2 \cdot (r,\varphi,\bar{T}) \text{ when } \bar{Z}\ =\ 0; \\ \dfrac{\partial\ \Theta}{\partial \bar{Z}}\ =\ g_3(r,\varphi,\bar{T}) \text{ when } \bar{Z}\ =\ l. \end{cases} \quad (5)$$

Here, the Green's function takes the following form:

$$G(r,\varphi,\bar{Z},\xi,\eta,\zeta,\bar{T})\ =\ \frac{\sin\left(\bar{T}\sqrt{|b|}\right)}{\pi R^2 l\sqrt{|b|}} + \frac{2}{\pi R^2 l} \cdot \sum_{k\,=\,1}^{\infty} \frac{1}{\sqrt{\beta_k}} \cdot \cos\left(\frac{k\pi\bar{Z}}{l}\right) \cdot \cos\left(\frac{k\pi\xi}{l}\right) \cdot \sin\left(\bar{T} \cdot \sqrt{\beta_k}\right) +$$

$$+\ \frac{1}{\pi l} \cdot \sum_{n\,=\,0}^{\infty} \sum_{m\,=\,1}^{\infty} \sum_{k\,=\,1}^{\infty} \frac{A_n \cdot A_k \cdot {\mu_{nm}}^2 \cdot I_n(\mu_{nm} r) \cdot I_n(\mu_{nm}\xi)}{({\mu_{nm}}^2 \cdot R^2 - n^2) \cdot [I_n(\mu_{nm} \cdot R)]^2} \cdot cos[n \cdot (\varphi - \eta)]\ \text{x} \quad (6)$$

$$\text{x}\ \cos\left(\frac{k\pi\bar{Z}}{l}\right) \cdot \cos\left(\frac{k\pi\xi}{l}\right) \cdot \frac{\sin\left(\lambda_{nmk} \cdot \bar{T}\right)}{\lambda_{nmk}}$$

$$\beta_k = \frac{v_t^2 \cdot k^2 \cdot \pi^2}{l^2} + b,$$

where $$\lambda_{nmk} = \sqrt{v_t^2 \cdot {\mu_{nm}}^2 + \frac{v_t^2 \cdot k^2 \cdot \pi^2}{l^2} + b}, A = \begin{cases} 1 \text{ when } n = 0; \\ 2 \text{ when } n > 0; \end{cases}$$

$I_n(\xi)$ – Bessel function of the argument (ξ); the bar above the function denotes the derivative with respect to that specific argument;
μ_{nm} – positive roots of the transcendental equation $I_n(\mu R) = 0$.

The domain is $0 \le r \le R$, $0 \le \varphi \le 2\,\pi$, $0 \le \bar{z} \le l$. Third boundary value problem. The following conditions are given:

$$\begin{cases} \Theta = f_0(r, \varphi, \bar{z}) \text{ when } \bar{T} = 0; \frac{\partial\,\Theta}{\partial \bar{T}} = f_1 \cdot (r, \varphi, \bar{z}) \text{ when } \bar{T} = 0; \\ \frac{\partial\,\Theta}{\partial r} + k_1 \cdot \Theta = g(\varphi, \bar{z}, \bar{T}) \text{ when } r = R; \\ \frac{\partial\,\Theta}{\partial \bar{Z}} - k_2 \cdot \Theta = g_2 \cdot (r, \varphi, \bar{T}) \text{ when } \bar{Z} = 0; \\ \frac{\partial\,\Theta}{\partial \bar{z}} + k_3 \cdot \Theta = g_3(r, \varphi, \bar{T}) \text{ when } \bar{Z} = l \end{cases} \quad (7)$$

The Green's function takes the following form:

$$G(r, \varphi, \bar{Z}, \xi, \eta, \zeta, \bar{T}) = \frac{1}{\pi} \cdot \sum_{n=0}^{\infty} \sum_{m=1}^{\infty} \sum_{k=1}^{\infty} \frac{A_n \cdot {\mu_{nm}}^2 \cdot I_n(\mu_{nm} r) \cdot I_n \cdot (\mu_{nm} \xi) \cdot cos[n \cdot (\varphi - \eta)]}{({\mu_{nm}}^2 \cdot R^2 + k_1^2 \cdot R^2 - n^2) \cdot [I_n(\mu_{nm} R)]^2} \cdot \frac{h_s(\bar{Z}) \cdot h_s(\zeta) \cdot sin(\lambda_{nmk} \cdot \bar{T})}{\|h_s\|^2 \lambda_{nms}}, \quad (8)$$

where

$$A = \begin{cases} 1 \text{ when } n = 0; \\ 2 \text{ when } n > 0; \end{cases}$$

$$\lambda_{nmk} = \sqrt{v_t^2 \cdot {\mu_{nm}}^2 + v_t^2 \cdot \beta_S^2 + b},$$

$$h_s(\bar{Z}) = \cos(\beta_S \cdot \bar{Z}) + \frac{k_2}{\beta_S} sin(\beta_S \cdot \bar{Z}),$$

$$\|h_s\|^2 = \frac{k_3}{2\beta_S^2} \cdot \frac{(\beta_s^2 - k_2^2)}{(\beta_S^2 - k_3^2)} + \frac{k_2}{2\beta_S^2} + \frac{l}{2}\left(1 + \frac{k_2^2}{\beta_S^2}\right)$$

$I_n(\xi)$ – Bessel function;
μ_{nm} and β_S – positive roots of the corresponding transcendental equations:

$$\mu \cdot I_n'(\mu R) + k_1 I_n(\mu R), \frac{tg(\beta l)}{\beta} = \frac{k_2 + k_3}{\beta^2 - k_2 \cdot k_3}.$$

Domain: $0 \le r \le R$, $0 \le \varphi \le 2\,\pi$, $0 \le \bar{z} \le l$. Mixed boundary value problems.

A. Given conditions:

$$\begin{cases} \Theta = f_0(r, \varphi, \bar{z}) \text{ when } \bar{T} = 0; \frac{\partial\,\Theta}{\partial \bar{T}} = f_1(r, \varphi, \bar{z}) \text{ when } \bar{T} = 0; \\ \Theta = g_1(\varphi, \bar{Z}, \bar{T}) \text{ when } r = R; \frac{\partial\,\Theta}{\partial \bar{Z}} = g_2(r, \varphi, \bar{T}) \text{ when } \bar{Z} = 0; \\ \frac{\partial\,\Theta}{\partial \bar{Z}} = g_3(r, \varphi, \bar{T}) \text{ when } \bar{Z} = l \end{cases} \quad (9)$$

Here, the Green's function takes the following form:

$$G(r,\varphi,\bar{Z},\xi,\eta,\zeta,\bar{T}) = \frac{1}{\pi R^2 l}\sum_{n=0}^{\infty}\sum_{m=1}^{\infty}\sum_{k=0}^{\infty}\frac{A_n\cdot A_k\cdot I_n(\mu_{nm}r)\cdot I_n(\mu_{nm}\xi)}{[I_n'(\mu_{nm}R)]^2\sqrt{\lambda_{nmk}}}\ \text{x}$$
$$\text{x}\ cos[n\cdot(\varphi-\eta)]\cdot\cos\left(\frac{k\pi\bar{Z}}{l}\right)\cdot\cos\left(\frac{k\pi\zeta}{l}\right)\cdot\sin\left(\bar{T}\cdot\sqrt{\lambda_{nmk}}\right), \quad (10)$$

where

$$\lambda_{nmk} = v_t^2\cdot{\mu_{nm}}^2 + \frac{v_t^2\cdot k^2\cdot\pi^2}{l^2} + b, A = \begin{cases}1 \text{ when } n = 0;\\ 2 \text{ when } n > 0;\end{cases}$$

$I_n(\xi)$ – Bessel function;

μ_{nm} – positive roots of the transcendental equation $I_n(\mu R) = 0$.

B. Given conditions:

$$\begin{cases}\Theta = f_0(r,\varphi,\bar{Z}) \text{ when } \bar{T} = 0;\ \frac{\partial\,\Theta}{\partial\bar{T}} = f_1(r,\varphi,\bar{Z}) \text{ when } t = 0;\\ \frac{\partial\,\Theta}{\partial r} = g_1(\varphi,\bar{Z},\bar{T}) \text{ when } r = R;\ \Theta = g_2(r,\varphi,\bar{T}) \text{ when } \bar{Z} = 0;\\ \Theta = g_3(r,\varphi,\bar{T}) \text{ when } \bar{Z} = l\end{cases} \quad (11)$$

In this case, the Green's function takes the following form:

$$G(r,\varphi,\bar{Z},\xi,\eta,\zeta,\bar{T}) = \frac{2}{\pi R^2 l}\cdot\sum_{k=1}^{\infty}\frac{1}{\sqrt{\beta_k}}\cdot\sin\left(\frac{k\pi\bar{Z}}{l}\right)\cdot\sin\left(\frac{k\pi\zeta}{l}\right)\cdot\sin\left(\bar{T}\cdot\sqrt{\beta_k}\right) +$$
$$+\frac{2}{\pi l}\cdot\sum_{n=0}^{\infty}\sum_{m=1}^{\infty}\sum_{k=1}^{\infty}\frac{A_n\cdot{\mu_{nm}}^2\cdot I_n(\mu_{nm}r)\cdot I_n(\mu_{nm}\xi)}{({\mu_{nm}}^2\cdot R^2-n^2)\cdot[I_n(\mu_{nm}\cdot R)]^2\cdot\sqrt{\lambda_{nmk}}}\ \text{x} \quad (12)$$
$$\text{x}\cos[n\cdot(\varphi-\eta)]\cdot\sin\left(\frac{k\pi\bar{Z}}{l}\right)\cdot\sin\left(\frac{k\pi\zeta}{l}\right)\cdot\sin\left(\bar{T}\cdot\sqrt{\lambda_{nmk}}\right)$$

where

$$\beta_k = \frac{v_t^2\cdot k^2\cdot\pi^2}{l^2} + b, \lambda_{nmk} = v_t^2\cdot{\mu_{nm}}^2 + \frac{v_t^2\cdot k^2\cdot\pi^2}{l^2} + b,$$
$$A = \begin{cases}1 \text{ when } n = 0;\\ 2 \text{ when } n > 0;\end{cases}$$

$I_n(\xi)$ – Bessel function;

μ_{nm} – positive roots of the transcendental equation $I_n'(\mu R) = 0$.

Analysis of the influence of the parameters of the rheological model of the heat transfer fluid flowing in a ground heat exchanger on the average flow velocity $\vec{U}$. For Shvedov-Bingham fluids, the average velocity U is determined using the Buckingham equation, and heat transfer is estimated using empirical relationships for Nusselt numbers at T_w = const. The Buckingham equation for this rheological model can be written in another form:

$$W = U = \frac{D\cdot\tau}{8\cdot\eta}\cdot\left[1-\frac{4\tau_0}{3\tau} + \frac{{\tau_0}^4}{3\tau^4}\right] \quad (13)$$

where $W = U$ – average flow velocity in the pipe for a given rheological model;

τ – shear stress, Pa;

τ_0 – dynamic yield shear stress, Pa;

η – plastic viscosity, Pa·s;

D – pipe diameter, m.

When calculating heat transfer for non-Newtonian fluids, the following empirical equations apply for calculating the average Nusselt number (Nu_{mid}) or its local value at the end of the pipeline (Nu):

$$Nu_{mid} = 1.75 \cdot \delta^{\frac{1}{3}}\{G(\bar{Z})\}^{\frac{1}{3}} \cdot \left(\frac{\mathfrak{r}}{\mathfrak{r}_m}\right)^{0.14}; \quad (14)$$

$$Nu = 1.20 \cdot \delta^{\frac{1}{3}}\{G(\bar{Z})\}^{\frac{1}{3}} \cdot \left(\frac{\mathfrak{r}}{\mathfrak{r}_m}\right)^{0.14}; \quad (15)$$

where $\mathfrak{r}$ – viscosity of the fluid at the average flow temperature (T_{mid});
$\mathfrak{r}_m$ – same but at the pipe wall;
$\delta = (3n' + 1)/(4n')$;
n' – fluid behavior index under conditions at the pipe wall;
$\{G \cdot (\bar{z})\} = Gc_p/(\lambda \cdot l)$ – Gretz number;
G – mass flow rate of the fluid, kg·h^{-1};
c_p – specific heat capacity of the fluid, J·kg^{-1}·K^{-1};
λ – thermal conductivity, W·m^{-1}·K^{-1};
l – length of the section for which the average Nusselt number (Nu_{mid}) or its local value at the end (Nu) is determined, m.

For an Ostwald-de Villiers pseudoplastic fluid [17], the average velocity U is expressed in terms of the pressure drop ΔP.

$$U = \frac{(S + 1)}{(S + 3)} \cdot \vartheta_{max} = \frac{(S + 1)}{(S + 3)} \cdot \frac{R}{(1 + S)} \cdot \left(\frac{R \cdot \Delta P}{2m \cdot l}\right)^{S}, S = \frac{1}{n}, \quad (16)$$

where $\Delta P = P_0 - P_1$ – pressure drop in the pipe (the difference in pressure at the inlet z = 0 and the outlet z = 1 of the pipe);
$K = m$ – fluid consistency.

Similarly, for the Ellis model [16-18], expressions for U have been derived that account for the viscosity parameters of the coolant at zero shear rate η_0 and the shear stress value at $\eta = \eta_0/2 - \tau_{1/2}$

$$U = \frac{1}{2} \cdot \vartheta_{max} \cdot \left[1 + \frac{4}{(3 + \propto)} \cdot \left(\frac{R \cdot \Delta P}{2l \cdot \tau_{0,5}}\right)^{\propto - 1}\right] / \left[1 + \frac{2}{(1 + \propto)} \cdot \left(\frac{R \cdot \Delta P}{2l \cdot \tau_{0,5}}\right)^{\propto - 1}\right], \quad (17)$$

where

$$\vartheta_{max} = \vartheta(z)|_{r=0} = \frac{R^2 \cdot \Delta P}{4l \cdot \eta_0} \cdot \left[1 + \frac{2}{(1 + \propto)} \cdot \left(\frac{R \cdot \Delta P}{2l \cdot \tau_{0,5}}\right)^{\propto - 1}\right].$$

In the case of non-isothermal flow of a pseudoplastic fluid, the velocity profile $v_z(r)$ and the average velocity U are determined using the zonal method or analytically for a constant behavior index n. When n = 1, the results agree with the standard formulas for a Newtonian fluid. For structurally viscous fluids ($Pr \gg 1$), the energy equation is solved in the boundary layer for the conditions T_w = const and q_w = const. Local and average Nusselt numbers are obtained. The local value of the Nusselt criterion and the average value of the Nusselt criterion over the length L for T_w = const:

$$Nu_x = 1.07(\bar{\chi} \cdot \tilde{P} \cdot \frac{D}{x})^{1/3}, \quad (18)$$

$$< Nu > = 1.62(\bar{\chi} \cdot \tilde{P} \cdot \frac{\mathrm{D}}{\mathrm{L}})^{1/3}. \quad (19)$$

The coefficient $\bar{\chi}$ accounts for the structural-viscous properties of the medium with linear (n = 1), quadratic (n = 2), and so on, flow laws.

The local value of the Nusselt criterion and the average value of the Nusselt criterion over the length L for q_w = const:

$$Nu_x = 1.29(\bar{\chi} \cdot \tilde{P} \cdot \frac{\mathrm{D}}{\mathrm{x}})^{1/3}, \quad (20)$$

$$< Nu > \; = \; 1.93(\bar{\chi} \cdot \tilde{P} \cdot \frac{\mathrm{D}}{\mathrm{L}})^{1/3}. \tag{21}$$

Thus, calculations show that the ratio of the heat transfer coefficients of fluids with structural viscosity to those of ordinary Newtonian fluids at identical values of $\tilde{P} \cdot D/L$ and under boundary conditions of both the first type T_w = const and the second type q_w = const will be:

$$Nu/Nu_0 \; = \; (\bar{\chi})^{1/3} \tag{22}$$

The value of $\bar{\chi}$, calculated for a series of structurally viscous fluids, did not exceed 1.3. Therefore, it should be expected that the values of the Nusselt criteria for such media under quasi-isothermal flow conditions will differ from their values for ordinary Newtonian fluids by no more than $\Delta = (Nu - Nu_0)/Nu_0 = Nu/Nu_0 - 1$. Table 1 lists the values of Nu/Nu_0 for various $\bar{\chi}$ and the corresponding Δ, %.

An analysis of the results presented in Table 1 shows that significant differences in (Nu/Nu_0) and Δ, % occur for fluids with structural viscosity, in which the coefficient $\bar{\chi}$ – which accounts for the structural-viscous properties of a medium with nonlinear flow laws – exceeds 3.0, because when $\bar{\chi} > 3.0$, $Nu/Nu_0 = 1.442... 2.714$, $\Delta = (44.2 \ldots 171.4)\%$. In this case, $\bar{\chi} \in [3.0; 20.0]$. Therefore, as a heat transfer fluid that carries heat in the pipeline, non-Newtonian viscous fluids with $\bar{\chi} \geq 3.0$ should be selected, which will significantly increase heat transfer from the soil surrounding the pipeline (by more than 44 to 172%).

Table 1

Values of the Nu/Nu_0 criterion; Δ, % for various $\bar{\chi}$.

$\bar{\chi}$.	Nu/Nu_0	Δ, %
1.5	1.1445	14.5
2.0	1.260	26.0
3.0	1.442	44.2
5.0	1.710	71.0
7.0	1.913	91.3
10.0	2.154	115.4
20.0	2.714	171.4

Energy efficiency of using tubular heat exchangers for high-viscosity non-Newtonian fluids. The energy assessment is based on relationships that characterize the rate of energy dissipation under varying properties. The direction of the heat flux is decisive in this case. When the coolant is heated, energy dissipation has a positive effect: the Nusselt numbers increase and hydraulic resistance decreases. During cooling, the effect is negative (Fig. 2). The following symbols are used in Fig. 2: $\bar{W}r_w$ – the average value of dissipated energy (caused by friction between layers of the heat transfer fluid) when the fluid comes into contact with the pipe walls; $\bar{K}$ – a coefficient that is a function of the Peclet number, the pipe diameter, and its length, i.e., $\bar{K} = (Pe, D, L)$; W_w – heat release from the wall; $\bar{W}$ – the average density of internal heat sources per unit volume.

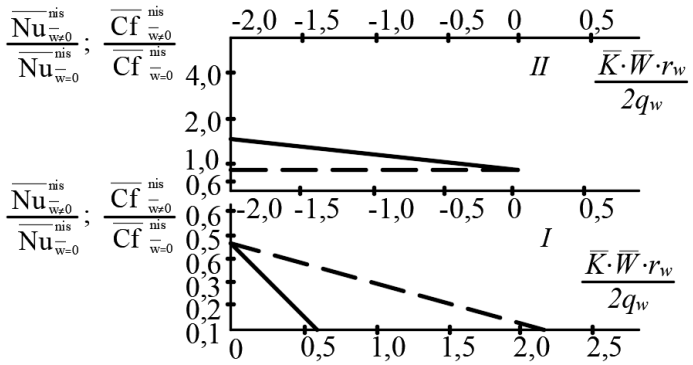

Fig. 2. **Effect of frictional heat (energy dissipation) on Nusselt numbers (solid curves) and hydraulic resistance coefficients C_f (dashed curves) at T_w = const (first-kind boundary conditions) for non-Newtonian fluids: I – cooling; II – heating**

For a quantitative assessment, the parameter k_o should be introduced, which is equal to the ratio of the amount of heat transferred to the energy expended for this purpose. It is precisely this parameter, albeit in a slightly modified form, that was used by the authors of [18; 19] for comparative evaluations of various heat exchange surfaces. The main advantage of this coefficient is that it characterizes the heat exchanger according to its direct technological purpose: to transfer heat with the minimum possible energy consumption. This coefficient k_o can be easily converted into a form convenient for analysis by using the approach from [20]:

$$k_Q = \frac{Pe \cdot \frac{D}{L}(1-\bar{\theta})}{32\left(\frac{\bar{c}_f^{nis}}{c_{fo}^{is\prime}}\right)Br_0^*}, \quad (23)$$

where Pe – Péclet number;

D – diameter of the pipeline, m;

L – length of the pipeline, m;

$\bar{c}_f^{nis}$ – average value of the hydraulic resistance coefficient under non-isothermal flow conditions;

$c_{fo}^{is\prime}$ – hydraulic resistance coefficient under isothermal flow conditions at the heat carrier inlet;

Br_0^* – Brinkman number determined using the parameters at the heat carrier inlet to the pipeline $Br_0^* = \mu_0^* \cdot \bar{U}^2/\lambda \cdot (T_0 - T_w)$

where μ_0^* – pseudoplastic viscosity of the heat carrier at the pipeline inlet, Pa·s;

$\bar{U}$ – average flow velocity over the circular cross-section of the pipeline, m·s^{-1};

T_0 – temperature at the pipeline inlet, °C;

$\bar{\theta} = (T - T_w)/(T_0 - T_w)$ – average mass (bulk) temperature.

From equation (23) it is clear that when $\bar{\theta} > 1$, $k_o < 0$, i.e. during cooling of the pipeline wall the liquid heats up and, accordingly, implementation of the process in the given direction is impossible. When $k_o < 1$ this process is energetically unprofitable, since the energy expenditure exceeds the amount of heat transferred. The results of determining k_o using formula (23) provide a clear illustration of the role of the heat flux direction, as well as the non-Newtonian properties of the heat carrier: plasticity and nonlinearity of the flow curve (Fig. 3).

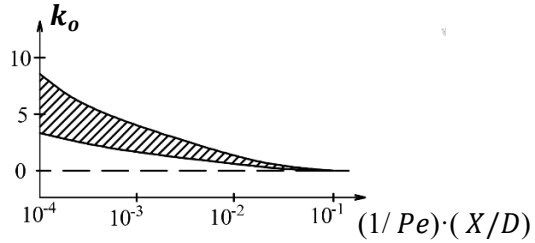

Fig. 3. **Dependence of k_o on pipe length for heat transfer conditions (first-kind boundary conditions T_w = const) when the coolant is heated**

For $Br_0^* \approx 0.5$ and at coolant flow rates and pipe diameters typically encountered in practice, the curves of the dependence $k_o = f((1/Pe)\cdot(X/D))$ lie within the range shaded in Fig. 3. That is, the parameter $(1/Pe)\cdot(X/D)$, where X is the length of the pipeline in the longitudinal direction along its axis, takes values from 10^{-4} to 10^{-2}, and k_o varies from 3…8 to 0. In the practical operation of ground-coupled tube heat exchangers, both types of boundary conditions are most commonly encountered. However, once the system has completed its break-in period and reached steady-state operation, the second type of boundary conditions more closely reflects the actual operating conditions. The third type of boundary conditions occurs at the beginning of the heat exchanger operating season, when conditions have not yet stabilized.

Conclusions

The Green's function was derived, and analytical solutions to the three-dimensional convective wave equation for a straight channel of a ground heat exchanger were obtained, taking into account the effect of internal coolant flow for boundary value problems of various types. A detailed analysis was conducted of the influence of the parameters of the coolant's rheological models (Shvedov–Bingham, Ostwald–de Villiers, Ellis, and structurally viscous fluid) on the average flow velocity and heat transfer intensity. It has been established that for structurally viscous fluids at $n > 3$, heat transfer increases by 44-172% compared to Newtonian fluids. The energy efficiency of tubular heat exchangers was evaluated using the $k_o$parameter. It has been established that when the heat transfer fluid is heated (T_w = const) and for typical values of $B_{r0}{}^* \approx 0.5$, the $k_o$parameter varies between 3 and 8 for small values of $(1/\ Pe)\cdot(\ X/D)$ (from 10^{-4} to 10^{-2}), which confirms the energy efficiency of the process. When the coolant is cooled, $k_o$becomes less than 1, making the process energetically unprofitable. Use straight-tube ground heat exchangers with a circular cross-section and constant diameter. Use non-linear structured fluids with a coefficient of $n \geq 3.0$ (e.g., propylene glycol-based nanofluids) as the heat transfer fluid. Operate primarily in heat transfer fluid heating mode at $B_{r0}{}^* \approx 0.5$. It is essential to account for the movement of the surrounding soil and dynamic operating modes (start-up, shutdown, reverse flow) when designing piping systems. Adhering to these recommendations allows for improved energy efficiency of heat pump systems for indoor sports facilities.

Author contributions

Conceptualization, Y.C.; methodology, A.M. and S.R.; software, Y.C.; validation, S.R. and P.Z.; formal analysis, Y.C. and A.M.; investigation, Y.C., A.M., S.R. and P.Z.; data curation, Y.C., A.M. and S.R.; writing – original draft preparation, Y.C.; writing – review and editing, A.M. and P.Z.; visualization, S.R. and P.Z.; project administration, A.M.; funding acquisition, P.Z. All authors have read and agreed to the published version of the manuscript.

References

[1] Tadić L., Čulo K. and Glavaš H. Performance analysis of a borehole thermal energy storage (BTES) system for seasonal heating. Energies, 15(18), 2022, p. 6847.
[2] Chovniuk Y., Moskvitina A., Shamych O. and Kholodova O. Synthesis of physical and mathematical model of energy-efficient microclimate management of rural area gym, taking into account indicators of comfort and air quality. Engineering for Rural Development, 24, 2025, pp. 706–715. Jelgava: Latvia University of Life Sciences and Technologies.
[3] Chovniuk Y., Moskvitina A., Shamych O., Rybachov S. and Kholodova O. Improvement of microclimate control energy-saving systems at indoor sports facilities in rural areas. Engineering for Rural Development, 24, 2025, pp. 764–771. Jelgava: Latvia University of Life Sciences and Technologies.
[4] Chovniuk Y., Moskvitina A., Rybachov S. and Zinych P. Nonisothermal flow of nanofluid in ground heat accumulator for decentralized heat supply of rural facilities for various purposes. Engineering for Rural Development, 23, Jelgava: Latvia University of Life Sciences and Technologies., 2024, pp. 623-629.
[5] Makarov V. L., Mayko N. V. and Ryabichev V. L. Realization of the Exact Three-Point Finite-Difference Schemes for the System of Second-Order Ordinary Differential Equations. Ukrainian Mathematical Journal, 75(1), 2023, pp. 80-106.
[6] Maleki A. and Zare S. Non-Newtonian Fluid Flow and Heat Transfer in Microchannels. International Journal of Heat and Mass Transfer, 195, 2023, 123140.
[7] Irgens F. Rheology and non-newtonian fluids. Vol. 1. New York: Springer International Publishing, 2014.
[8] Ochs F., Dalla Rosa A. and Svendsen S. The role of borehole thermal energy storage in district heating systems: A case study in Denmark. Energy, 2021, 121543.
[9] Fischer J. and Stephens D. Aerodynamic sound generation in pipe systems: modern analytical approaches. AIAA Journal, 61(4), 2023, pp. 1512-1528.
[10] Morgans A. S. Duran I. Entropy noise in aeroacoustics: Waves, flows and modeling. Annual Review of Fluid Mechanics, 54, 2022, pp. 111-135.

[11] Lighthill J. Informal Introduction to Theoretical Fluid Mechanics. Oxford University Press, 2021.
[12] Borysiuk A. O. Sound generation by a localized region of disturbed flow in a rigid-walled cylindrical pipe with a fluid flow. Journal of Sound and Vibration, 468, 2020, 115096.
[13] Borysiuk A. O. Green's functions for the convective wave equation in a rectangular duct with flow. Journal of Sound and Vibration, 455, 2019, pp. 120-135.
[14] Borysiuk A. O. Green's functions of the convective wave equation for a rigid rectangular pipe. Journal of Mathematical Sciences, 230(3), 2018, pp. 374-388.
[15] Borysiuk A. O. Three-dimensional Green's function for the convective wave equation in a duct. Acoustical Physics (International Edition), 66, 2020, pp. 1-12.
[16] Abe T. and Brown P. Transport Phenomena: A Modern Approach to Momentum, Heat, and Mass Transfer. Cambridge University Press, 2021.
[17] González R., Tamburrino A., Vacca A. and Iervolino M. Pulsating Flow of an Ostwald – De Waele Fluid between Parallel Plates. Water, 12(4), 2020, 932.
[18] Siginer D. A. Developments in the Flow of Complex Fluids in Tubes. Springer International Publishing, 2015.
[19] Poole R. J. Inelastic and flow-type parameter models for non-Newtonian fluids. Journal of Non-Newtonian Fluid Mechanics, 320, 2023, 105106.
[20] Quemada D. Rheological modelling of complex fluids. I. The concept of effective volume fraction revisited. The European Physical Journal-Applied Physics, 1(1), 1998, pp. 119-127.